Experimental Realization of a Magnetic Cloak

Fedor Gömöry *et al.*

Science **335**, 1466 (2012);
DOI: 10.1126/science.1218316

Science (print ISSN 0036-8075; online ISSN 1095-9203) is published weekly, except the last week in December, by the American Association for the Advancement of Science, 1200 New York Avenue NW, Washington, DC 20005.

$A_{d(f)}$, $B_{d(f)}$, $C_{d(f)}$, and $D_{d(f)}$ are parameters, and $\mathbf{J}_{3/2}$ are spin matrices for angular momentum 3/2. The first three terms have continuous rotational symmetry; the last term breaks continuous rotational symmetry while preserving cubic symmetry, which is responsible for the band inversion only along Γ-*X* direction rather than other directions in the BZ (*25*). The off-diagonal Hamiltonian H_{df} connects d and f bands of opposite parities; therefore, the first-order term can be written as

$$H_{df} = iF(k_x\{J_{3/2}{}^y, J_{3/2}{}^z\} + k_y\{J_{3/2}{}^z, J_{3/2}{}^x\} + k_z\{J_{3/2}{}^x, J_{3/2}{}^y\}) \quad (3)$$

F is a parameter, and the notation $\{A, B\} = (AB + BA)/2$ denotes the symmetrized product of its arguments. The above effective model preserves time-reversal and inversion symmetry.

Because the 5f and 6d orbitals are localized, we only consider the nearest neighborhood hopping of Am-Am and Pu-Pu atoms. Each Am (Pu) atom has 12 nearest neighbors located at $\pm\mathbf{a}_1$, $\pm\mathbf{a}_2$, $\pm\mathbf{a}_3$, $\pm(\mathbf{a}_2 - \mathbf{a}_1)$, $\pm(\mathbf{a}_2 - \mathbf{a}_3)$, and $\pm(\mathbf{a}_3 - \mathbf{a}_1)$. So we can extend the above continuum model to the TB lattice model and reproduce the low-energy bands of these materials well, with AmN as an example (*25*). Two important effects of the U interaction are to renormalize the SOC parameters between $5f^{5/2}$ and $5f^{7/2}$states and to induce a metal-insulator transition. On the insulator side, we can effectively fit our eight-by-eight Hamiltonian in the single-particle picture with parameters renormalized by U to the LDA+U first-principle calculations.

To identify the surface states, we perform an ab initio calculation for the semi-infinite AmN system with open boundary condition in the "+z" direction on the basis of maximally localized Wannier functions (MLWFs) (*27*, *28*). We can obtain the surface Green's function of the semi-infinite system iteratively. Lastly, the local density of states (LDOS) can be calculated with the imaginary part of these Green's functions. From these LDOS, we can obtain the dispersion of the surface states, (Fig. 2C). A single Dirac cone at $\bar{\Gamma}$ shows up in the energy gap, which demonstrates the nontrivial Z_2 topology of the material in addition to the parity analysis. The Fermi velocity for the Dirac cone is $v_F \cong 1.3 \times 10^5$ m/s, a little smaller than Bi_2Se_3 (*23*). To confirm this result, we also take the open boundary condition in z direction in the analytical TB model (*25*), which yields the same single Dirac cone surface state at Γ point of the BZ as in the ab initio calculation.

This work could lead to the discovery of more interacting TI materials in the actinide family. The topological surface states in actinide materials would offer better ways to optimize electrical and thermal transport properties, leading to novel designs for nuclear energy applications.

References and Notes

1. X. L. Qi, S. C. Zhang, *Phys. Today* **63**, 33 (2010).
2. X. L. Qi, S. C. Zhang, *Rev. Mod. Phys.* **83**, 1057 (2011).
3. M. Z. Hasan, C. L. Kane, *Rev. Mod. Phys.* **82**, 3045 (2010).
4. B. A. Bernevig, T. L. Hughes, S. C. Zhang, *Science* **314**, 1757 (2006).
5. S. Raghu, X. L. Qi, C. Honerkamp, S. C. Zhang, *Phys. Rev. Lett.* **100**, 156401 (2008).
6. X. L. Qi, R. D. Li, J. D. Zang, S. C. Zhang, *Science* **323**, 1184 (2009); 10.1126/science.1167747.
7. L. Fu, C. L. Kane, *Phys. Rev. Lett.* **100**, 096407 (2008).
8. R. D. Li, J. Wang, X. L. Qi, S. C. Zhang, *Nat. Phys.* **6**, 284 (2010).
9. K. T. Moore, G. van der Laan, *Rev. Mod. Phys.* **81**, 235 (2009).
10. T. Gouder, P. M. Oppeneer, F. Huber, F. Wastin, J. Rebizant, *Phys. Rev. B* **72**, 115122 (2005).
11. D. B. Ghosh, S. K. De, P. M. Oppeneer, M. S. S. Brooks, *Phys. Rev. B* **72**, 115123 (2005).
12. S. Suzuki, T. Ariizumi, *J. Phys. Soc. Jpn.* **76**, 024707 (2007).
13. M.-T. Suzuki, P. M. Oppeneer, *Phys. Rev. B* **80**, 161103 (2009).
14. V. Ichas, J. C. Griveau, J. Rebizant, J. C. Spirlet, *Phys. Rev. B* **63**, 045109 (2001).
15. M. S. S. Brooks, *J. Magn. Magn. Mater.* **63-64**, 649 (1987).
16. Z. Fang, K. Terakura, *J. Phys. Condens. Matter* **14**, 3001 (2002).
17. D. Vanderbilt, *Phys. Rev. B* **41**, 7892 (1990).
18. V. I. Anisimov, I. V. Solovyev, M. A. Korotin, *Phys. Rev. B* **48**, 16929 (1993).
19. V. I. Anisimov, J. Zaanen, O. K. Andersen, *Phys. Rev. B* **44**, 943 (1991).
20. F. Wastin, J. C. Spirlet, J. Rebizant, *J. Alloy. Comp.* **219**, 232 (1995).
21. M. S. Dresselhaus, G. Dresselhaus, A. Jorio, *Group Theory Application to the Physics of Condensed Matter* (Springer, Berlin, 2008).
22. M. Dzero, K. Sun, P. Coleman, V. Galitski, *Phys. Rev. B* **85**, 045130 (2012).
23. H. J. Zhang *et al.*, *Nat. Phys.* **5**, 438 (2009).
24. L. Fu, C. L. Kane, *Phys. Rev. B* **76**, 045302 (2007).
25. Materials and methods are available as supporting material on *Science* Online.
26. J. M. Luttinger, *Phys. Rev.* **102**, 1030 (1956).
27. N. Marzari, D. Vanderbilt, *Phys. Rev. B* **56**, 12847 (1997).
28. I. Souza, N. Marzari, D. Vanderbilt, *Phys. Rev. B* **65**, 035109 (2001).
29. B. Kanellakopulos, J. P. Charvillat, F. Maino, W. Muller, *Transplutonium 1975* (North-Holland, Amsterdam, 1976).

Acknowledgments: We thank S. Raghu for useful discussions. This work is supported by the U.S. Department of Energy, Office of Basic Energy Sciences, Division of Materials Sciences and Engineering, under contract DE-AC02-76SF00515 and in part by the Army Research Office under the grant number W911NF-09-1-0508.

Supporting Online Material

www.sciencemag.org/cgi/content/full/335/6075/1464/DC1
Materials and Methods
SOM Text
Fig. S1
Tables S1 and S2
References (*30*, *31*)

3 November 2011; accepted 17 February 2012
10.1126/science.1216184

Experimental Realization of a Magnetic Cloak

Fedor Gömöry,[1] Mykola Solovyov,[1] Ján Šouc,[1] Carles Navau,[2] Jordi Prat-Camps,[2] Alvaro Sanchez[2]*

Invisibility to electromagnetic fields has become an exciting theoretical possibility. However, the experimental realization of electromagnetic cloaks has only been achieved starting from simplified approaches (for instance, based on ray approximation, canceling only some terms of the scattering fields, or hiding a bulge in a plane instead of an object in free space). Here, we demonstrate, directly from Maxwell equations, that a specially designed cylindrical superconductor-ferromagnetic bilayer can exactly cloak uniform static magnetic fields, and we experimentally confirmed this effect in an actual setup.

Rendering an object in free space invisible has important scientific and technological implications. Invisibility at several frequencies, including visible light, has started to be an actual possibility (*1*–*4*). Most cloak designs, however, require extreme (anisotropic, spatially inhomogeneous, and even singular) values of magnetic permeability μ and electric permittivity ε. They also involve other more fundamental problems, such as superluminal phase velocities and extremely narrow bandwidths (*5*, *6*). Whereas cloaks based on plasmonics are free from some of these limitations, they are achieved at the price of giving up exact invisibility by canceling only some scattering terms (*4*).

Some experimental works have attempted to achieve cloaking, albeit in reduced schemes; that is, giving up exactness for the sake of feasibility. In recent work by Schurig *et al*. (*7*), the goal was not to render a full cloak but a reduced scheme, with some reflection and shadowing. Resonant metamaterials in the microwave frequency were used, which had a narrow frequency band with a relatively large loss (*8*). A plasmonic approach was also experimentally demonstrated (*9*) in which the scattering of a particular dielectric object was decreased but not eliminated. Another strategy to reduce a full cloaking scheme into something more practical is the carpet cloak (*10*, *11*), with several experimental realizations, even in the optical range (*12*–*14*), although they attempt to hide

[1]Institute of Electrical Engineering, Slovak Academy of Sciences, Slovakia. [2]Grup d'Electromagnetisme, Departament de Física, Universitat Autònoma de Barcelona, 08193 Bellaterra, Barcelona, Catalonia, Spain.

*To whom correspondence should be addressed. E-mail: alvar.sanchez@uab.cat

a bulge instead of a three-dimensional object in free space (*12*).

The definitive confirmation of cloaking requires finding a system that (i) can be theoretically derived as an exact cloak from first principles (not a reduced scheme) and (ii) can be experimentally realized with existing materials; for example, those made only of nonsingular, homogeneous, and isotropic materials.

We show in this work that for static magnetic fields one can design a scheme fulfilling (i) and (ii), as mentioned above. Our scheme consists of a long cylinder with two concentric layers made of homogeneous isotropic materials: an inner superconducting (SC) one, which expels magnetic fields (ideally considered as a zero-permeability material), and an outer ferromagnetic (FM) one. An exact cloak behavior of uniform static magnetic fields for such a bilayer will be analytically demonstrated directly based on Maxwell equations. Cloaking static magnetic fields has the important advantage that the magnetic and electric effects decouple and only the magnetic permeabilities need to be considered. A scheme to cloak static magnetic fields was proposed (*15*–*17*) based on transformation optics (*1*) [note that the scheme in (*2*) is valid only on scales much larger than the wavelength, so is not applicable to dc cloaking], but it required extreme values of permeabilities. An approximate design based on discrete layers has recently been presented (*18*).

Based on Maxwell equations, we show [see supporting online material (SOM) text] that a bilayer consisting of an infinitely long cylindrical superconducting shell of interior and exterior radii R_0 and R_1, respectively, surrounded by another cylindrical magnetic shell (with constant permeability μ_2) of interior and exterior radii R_1 and R_2, respectively (Fig. 1C), exactly cloaks a uniform magnetic field when the permeability of the outer layer follows

$$\mu_2 = \frac{R_2^2 + R_1^2}{R_2^2 - R_1^2} \qquad (1)$$

Equation 1 represents a whole family of solutions, depending on μ_2 and the ratio R_2/R_1. A similar bilayer structure also exactly cloaks static uniform magnetic fields in a sphere (SOM text). Moreover, when the applied field is nonuniform, the field distortion outside the bilayer is relatively small and can be reduced by adjusting the thickness of the layers (SOM text).

For nonzero frequency electromagnetic waves, the interaction between electric and magnetic fields complicates the control of light. Controlling static magnetic fields is simpler: Materials exist in nature with permeabilities $\mu > 1$ and $\mu < 1$ that attract and repel magnetic flux lines, respectively (Fig. 1, A and B). Our bilayer (Fig. 1C) is based on the existence of an exact solution that provides the right combination of repelling (inner SC layer) and attracting (outer FM layer) magnetic field lines so as to cancel any external distortion.

An important property of our bilayer is that placing a superconductor as the inner layer ensures that an external field does not penetrate inside the cylinder (*18*, *19*) and that the field of a magnetic source inside the cloak will not leak outside (*18*). So the challenging task is to experimentally demonstrate the zero external-field distortion.

We fabricated a SC-FM bilayer (Fig. 2A). Instead of uniform superconducting and ferromagnetic cylinders proposed in the ideal bilayer, the inner superconducting shell consisted of a few turns of high-temperature superconductor tape (*20*), and the outer layer was composed of a few turns of a thick FeNiCr commercial alloy sheet (*21*). The magnetic response of the bilayer in a uniform applied field of 40 mT generated by a split pair of race-track electromagnets was measured using an existing experimental setup, utilized before for measuring superconducting tapes (*22*), which provided the required accuracy and calibration in magnetic and position measurements but did not allow for measuring of long cylinders. We obtained good cloaking results, even though the cylindrical bilayer was relatively short. We mapped the vertical component of magnetic field (y component) with a Hall probe in the median plane of the bilayer along the lines transversal to its axial length (green dotted lines in Fig. 1). Such an experiment was performed in three different cases: (i) FM only at room temperature (i.e., superconducting tape over the critical temperature, thus electromagnetically inactive); (ii) SC only at 77 K, after unwinding the outer FM shell, to see the reference case of only the inner superconducting shell; and (iii) SC-FM bilayer at 77 K, the anticipated operating condition for magnetic invisibility.

The calculated vertical component of the magnetic field along the dotted lines in Fig. 1 corresponding to the three cases is plotted in Fig. 3A, assuming an exact bilayer with ideal parameters and the dimensions used in the experiments. The superconductor and the ferromagnet repel and attract field lines so the vertical component of the magnetic field in the central region tends to be smaller and larger than the applied field, respectively. For our bilayer, the combined response yields only the vertical component of the applied field (no field distortion).

The results of our experiments (Fig. 3, B and C) show that the magnetic signature of our bilayer cloak practically leaves the applied field of 40 mT unaffected and is weaker than the cases of only the SC or only the FM layer. Some small deviations appear in the experiments, possibly resulting from the short length of the bilayer (comparable to its diameter), so that the magnetic flux can also avoid the object in more directions, as well as the nonideal behavior of the SC and FM layers (*21*). Experimental results did not change with the rotation of the bilayer around its longitudinal axis. The observed suppression of magnetic signature was also substantial at some distance

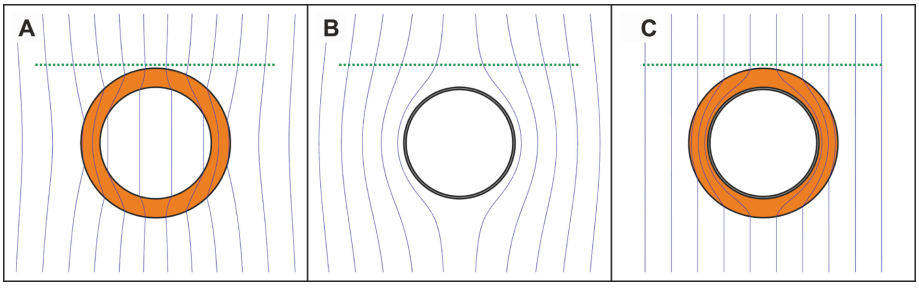

Fig. 1. Calculated field lines for (**A**) a single cylindrical magnetic shell with $\mu = 3.54$, attracting fields and having some field penetration in its interior; (**B**) a single cylindrical superconducting shell with $\mu = 0$ repelling field lines; and (**C**) a cylindrical bilayer with an inner superconducting layer ($\mu = 0$) of interior (exterior) radius of $R_0 = 0.96\ R_1$ (R_1) and an outer magnetic layer with $R_2/R_1 = 1.34$ with $\mu_2 = 3.54$, fulfilling Eq. 1. These values are chosen to approximate those used in the experiments. Green dotted lines denote the measuring lines in the experiments.

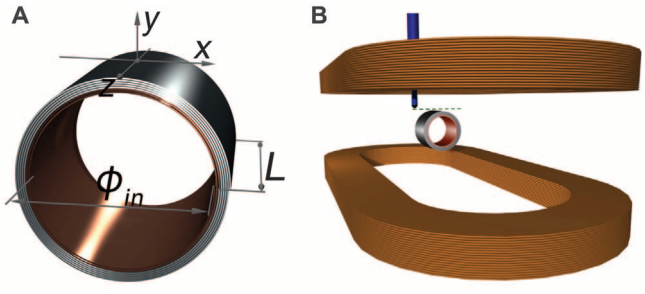

Fig. 2. (**A**) Scheme of the experimental magnetic cloak consisting of two shells: The inner one (brown) is made of several turns of superconducting tape, and several turns of tape with ferromagnetic properties create the outer shell (gray). In our case, length $L = 12$ mm and diameter $\phi_{in} = 12.5$ mm. Preparation of such structure requires a cylindrical former (not shown in the image). (**B**) Experimental setup for mapping the magnetic field in the vicinity of the magnetic cloak. The magnetic field is generated by a pair of race-track coils wound from Cu wire (brown). The Hall probe is mounted on the bottom of the holder rod (blue).

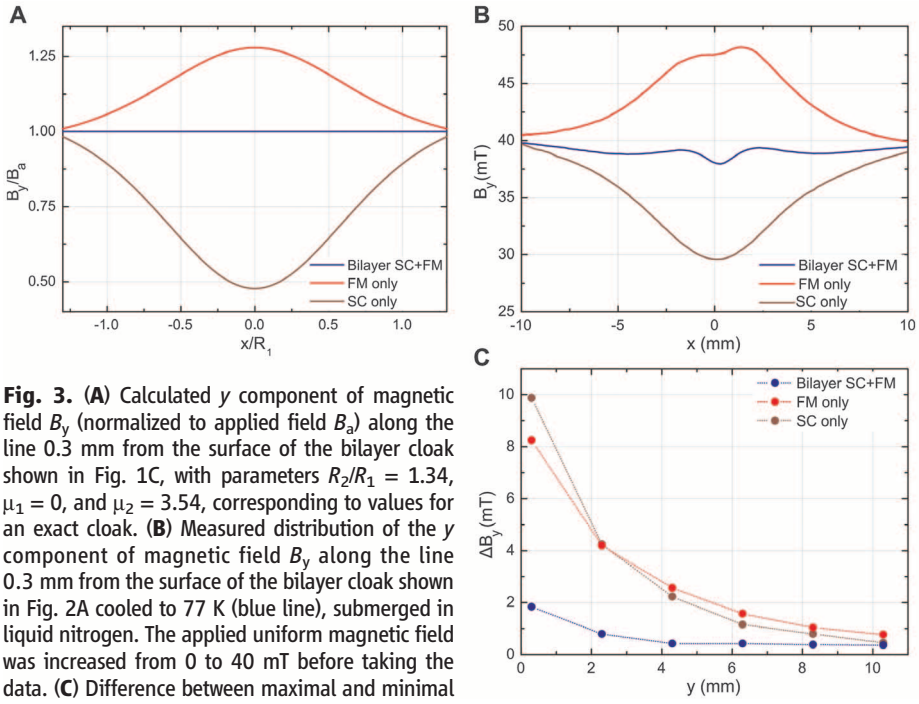

Fig. 3. (**A**) Calculated *y* component of magnetic field B_y (normalized to applied field B_a) along the line 0.3 mm from the surface of the bilayer cloak shown in Fig. 1C, with parameters $R_2/R_1 = 1.34$, $\mu_1 = 0$, and $\mu_2 = 3.54$, corresponding to values for an exact cloak. (**B**) Measured distribution of the *y* component of magnetic field B_y along the line 0.3 mm from the surface of the bilayer cloak shown in Fig. 2A cooled to 77 K (blue line), submerged in liquid nitrogen. The applied uniform magnetic field was increased from 0 to 40 mT before taking the data. (**C**) Difference between maximal and minimal values of the *y* component of magnetic field B_y for scans taken from $x = -10$ to 10 mm at various heights *y*. (A to C) Red line, FM only (in experiments obtained at room temperature; i.e., superconductor inactive); deep red line, SC only (experimentally, after removing the ferromagnetic layers); blue line, data for the SC-FM bilayer.

from the object, as seen from mapping at different vertical heights above the surface (Fig. 3C).

Both the SC and FM layers have been widely used independently of one another for magnetic shielding (*23*); our results show that the right combination of them yields shielding with no external-field distortion. Because in our static case there is no wavelength limiting the size of the objects, which differs from cloaks at other frequencies, our results can be naturally scaled up or down to any size of interest.

Because our cloak design for uniform magnetic field does not rely on transformation optics (*24*, *25*), problems present in previous cloaking proposals, such as superluminial velocity and singular parameters (*6*, *24*, *26*), are avoided. Also, the starting exact cloak means that scattering fields are zero and not only the dominant orders as in the scattering-cancellation technique based on plasmonics (*4*). Thus, our magnetic bilayer in a uniform magnetic field is an ideal case for full confirmation of cloaking ideas. Because the imperfection in the cloaking results not from intrinsic reasons but from the simplicity of the experiments, further experimental refinements will better approach the theoretical exact-field cancellation. Finally, our results were obtained using only commercially available materials, for fields as large as 40 mT, and at liquid-nitrogen temperatures, indicating that our ideas may be readily applied to technology.

References and Notes

1. J. B. Pendry, D. Schurig, D. R. Smith, *Science* **312**, 1780 (2006).
2. U. Leonhardt, *Science* **312**, 1777 (2006).
3. A. Greenleaf, M. Lassas, G. Uhlmann, *Physiol. Meas.* **24**, 413 (2003).
4. A. Alù, N. Engheta, *J. Opt. A Pure Appl. Opt.* **10**, 093002 (2008).
5. J. Perczel, T. Tyc, U. Leonhardt, *N. J. Phys.* **13**, 083007 (2011).
6. P. Alitalo, F. Bongard, J.-F. Zürcher, J. Mosig, S. Tretyakov, *Appl. Phys. Lett.* **94**, 014103 (2009).
7. D. Schurig *et al.*, *Science* **314**, 977 (2006).
8. H. F. Ma, T. J. Cui, *Nat. Commun.* **1**, article 21 (2010).
9. B. Edwards, A. Alù, M. Silveirinha, N. Engheta, *Phys. Rev. Lett.* **103**, 153901 (2009).
10. J. Li, J. B. Pendry, *Phys. Rev. Lett.* **101**, 203901 (2008).
11. R. Liu *et al.*, *Science* **323**, 366 (2009).
12. X. Chen *et al.*, *Nat. Commun.* **2**, article 176 (2011).
13. T. Ergin, N. Stenger, P. Brenner, J. B. Pendry, M. Wegener, *Science* **328**, 337 (2010).
14. B. Zhang, Y. Luo, X. Liu, G. Barbastathis, *Phys. Rev. Lett.* **106**, 033901 (2011).
15. B. Wood, J. B. Pendry, *J. Phys. Condens. Matter* **19**, 076208 (2007).
16. F. Magnus *et al.*, *Nat. Mater.* **7**, 295 (2008).
17. C. Navau, D.-X. Chen, A. Sanchez, N. Del-Valle, *Appl. Phys. Lett.* **94**, 242501 (2009).
18. A. Sanchez, C. Navau, J. Prat-Camps, D.-X. Chen, *New J. Phys.* **13**, 093034 (2011).
19. J. J. Rabbers, M. P. Oomen, E. Bassani, G. Ripamonti, G. Giunchi, *Supercond. Sci. Technol.* **23**, 125003 (2010).
20. Y. Xie, K. Tekletsadik, D. Hazelton, V. Selvamanickam, *IEEE Trans. Appl. Supercond.* **17**, 1981 (2007).
21. Materials and methods are available as supporting material on *Science* Online.
22. M. Solovyov, F. Gömöry, *IEEE Trans. Appl. Supercond.* **21**, 3277 (2011).
23. J. Vrba, S. E. Robinson, *Methods* **25**, 249 (2001).
24. H. Chen, C. T. Chan, P. Sheng, *Nat. Mater.* **9**, 387 (2010).
25. V. M. Shalaev, *Science* **322**, 384 (2008).
26. U. Leonhardt, *Nature* **471**, 292 (2011).

Acknowledgments: We thank D.-X. Chen for valuable comments and Consolider Project NANOSELECT (CSD2007-00041) and VEGA 2/0172/09 for financial support.

Supporting Online Material

www.sciencemag.org/cgi/content/full/335/6075/1466/DC1
Materials and Methods
SOM Text
Figs. S1 to S4
References (*27*–*33*)

22 December 2011; accepted 8 February 2012
10.1126/science.1218316

Renewable Cathode Materials from Biopolymer/Conjugated Polymer Interpenetrating Networks

Grzegorz Milczarek[1] and Olle Inganäs[2]*

Renewable and cheap materials in electrodes could meet the need for low-cost, intermittent electrical energy storage in a renewable energy system if sufficient charge density is obtained. Brown liquor, the waste product from paper processing, contains lignin derivatives. Polymer cathodes can be prepared by electrochemical oxidation of pyrrole to polypyrrole in solutions of lignin derivatives. The quinone group in lignin is used for electron and proton storage and exchange during redox cycling, thus combining charge storage in lignin and polypyrrole in an interpenetrating polypyrrole/lignin composite.

Renewable energy systems based on intermittent sources require methods for power balancing over time, and thus some means of storage. Charge storage in organic polymers rarely gives energy and power densities, gravimetric or volumetric, that match the needs for secondary batteries and supercapacitors. This was one reason for the abandonment of efforts to make polymer batteries from conjugated polymers two decades ago (*1*), because inorganic insertion electrodes are superior. Widespread application of electrical power storage may require more abundant materials than those available in inorganics (which often require rare metals), and